

# Computing Photonic Eigen-Modes and Bandwidth for 1D Photonic Crystal with Different Material Compositions

Sourangsu Banerji<sup>1</sup>, Arpan Deyasi<sup>2</sup>

<sup>1</sup>Programmer Analyst, Cognizant Technology Solutions, Kolkata; INDIA

<sup>2</sup>Assistant Professor, Department of Electronics & Communication Engineering, RCC Institute of Information Technology, Kolkata-700015; INDIA

<sup>1</sup>sourangsu.banerji@gmail.com; <sup>2</sup>deyasi\_arpan@yahoo.co.in

## Abstract

*In this paper, eigenmodes of one-dimensional multilayer photonic crystal structure is analytically computed using transfer matrix technique. Refractive index contrast ratio is calculated along with reflectivity and transmittivity as a function of indices assuming direction of wave propagation is along the confinement. Photonic bandwidth is computed under weak and strong coupling conditions between forward and backward propagating waves for different material systems. Result shows that width of photonic bandgap increases with increasing the contrast ratio. Simulation is useful for experimental researchers to determine the bandwidth centered at 1550 nm for sole purpose of optical communication.*

**Keyword(s):** Eigenmode, Photonic crystal, Transfer matrix technique, Refractive index contrast ratio, Photonic bandwidth, Material composition

## 1. Introduction

Propagation of electromagnetic wave through the structures with periodicities along the direction of confinement suffers dispersive effects. This is already exhibited in photonic crystal where permittivity of the dielectric material undergo periodic changes, result in photonic bandgap [1-2]. This unique property helps to block the propagation of some wavelength, and allows other spectra; thus can effectively be considered as optical bandpass filter [3]. This phenomenon can be explained by the principle of Bragg's reflection [4], where we assume that wavelength of light will be of the order of layer dimensions [5]. Materials exhibit photonic bandgap can be used in designing photonic crystal fiber [6], which may replace the conventional optical fiber due to its highly improved performance from communication point-of-view [7]. It is used to construct optical transmitter [8], switch [9], waveguide [10] etc.

Bandgap of 2D photonic crystal is studied by varying column roundness by Hillebrand [11] using plane-wave expansion method. Recently, finite-difference-time-domain method is used to analyze the forbidden region of photonic crystal with different geometries [12]. Zhao calculated the width of bandgap [13] using Bragg's principle of reflection. Men optimized the computational problem using semi-definite programming and subspace methods [14]. Evolutionary algorithm [15] and level-set method [16] are also used for design of large bandgap crystal.

The organization of this paper is as follows; section 2 consists of rigorous calculation of refractive index contrast ratio using transfer matrix technique, section 3 discusses the simulated results for different material systems under weak and strong coupling conditions. Lastly we conclude our paper.

## 2. Mathematical Modeling

We consider a multilayer planar structure characterized by a transfer matrix  $T$  which is a product of the transfer matrices of all the layers given by Eq. (13). The solutions of the Maxwell's equations are the photonic eigenmodes of the structure characterized by the following boundary condition: no light is incident on the structure from the left-hand side ( $z \rightarrow -\infty$ ) as well as from the right-hand side ( $z \rightarrow +\infty$ ). Thus, the electric field of the eigenmode at  $z \rightarrow -\infty$  can be represented as

$$\vec{E}_0 e^{ik_x x + ik_y y + ik_z z} \quad (1)$$

with  $\text{Re}(k_z) \geq 0$ ,  $\text{Im}(k_z) \leq 0$ , while at  $z \rightarrow +\infty$  the electric field can be represented with  $\text{Re}(k_z) \leq 0$ ,  $\text{Im}(k_z) \geq 0$ .

In TE-polarization, let us choose the system of coordinates in such a way that electric and magnetic field of the light mode are oriented as follows:

$$\vec{E} = \begin{pmatrix} 0 & E_y & 0 \end{pmatrix} \quad (2.1)$$

$$\vec{B} = \begin{pmatrix} B_x & 0 & B_z \end{pmatrix} \quad (2.2)$$

Transfer matrix  $T_{TE}$  now links the vectors  $E_y$  and  $B_x$  at the left-hand and right-hand boundaries of the structure, so we get

$$\hat{T}_{TE} \begin{pmatrix} E_y^{left} \\ B_x^{left} \end{pmatrix} = \begin{pmatrix} E_y^{right} \\ B_x^{right} \end{pmatrix} \quad (3)$$

Substituting the expression of the electric field, into the first of Maxwell's equations gives us

$$\frac{k_z}{k_0} E_y = B_x \quad (4)$$

where  $k_0 = \omega/c$ .

This allows us to rewrite Eq. (3) as

$$\hat{T}_{TE} \begin{pmatrix} 1 \\ \frac{k_z^{left}}{k_0} \end{pmatrix} = A \begin{pmatrix} 1 \\ \frac{k_z^{right}}{k_0} \end{pmatrix} \quad (5)$$

where  $k_z^{left}$  and  $k_z^{right}$  are  $z$ -components of the wave-vector of light on the left as well as the right sides of the structure correspondingly. Excluding  $A$  in Eq. (5), the equation can be easily reduced to a single transcendental equation giving the eigen-modes of the structure:

$$t_{11}^{TE} \frac{k_z^{right}}{k_0} + t_{12}^{TE} \frac{k_z^{left} k_z^{right}}{k_0^2} - t_{21}^{TE} - \frac{k_z^{left}}{k_0} t_{22}^{TE} = 0 \quad (6)$$

where  $t_{ij}$  are elements of the transfer matrix  $T_{TE}$ . We should keep in mind that the solutions of Eq. (6) are really complex frequencies in the general sense. However, only those which are characterized by a positive real part as well as a negative (or zero) imaginary part have a physical sense. The imaginary part of eigen-frequency is inversely proportional to the total life-time of the eigenmode. The equation for TM-polarized modes eigen-frequencies can be obtained in a similar way, which is

$$t_{11}^{TM} \frac{k_z^{right}}{n_{right}^2 k_0} + t_{12}^{TM} \frac{k_z^{left} k_z^{right}}{n_{left}^2 n_{right}^2 k_0^2} - t_{21}^{TM} - \frac{k_z^{left}}{n_{left}^2 k_0} t_{22}^{TM} = 0 \quad (7)$$

Under the condition of normal incidence, equations for the photonic eigenmodes in both TE- and TM-polarizations, namely Eq. (6) and Eq. (7) become formally identical.

Using suitable transformations, these equations can be reduced in the forms

$$t_{11} n_{right} - t_{12} n_{right} n_{left} - t_{21} + n_{left} t_{22} = 0 \quad (8)$$

with  $t_{ij}$  being element of the transfer matrix at normal incidence.

Assuming dependence of the structure  $z$  coordinate is a periodic function with period  $d$ , we consider transfer matrix  $T_d$  across the period of the structure may be written as a product of a finite number of matrices. Considering electromagnetic wave propagate along the  $z$ -direction, we can write,

$$\hat{T}_d \vec{\Phi}|_{z=0} = \vec{\Phi}|_{z=d} \quad (9)$$

where  $\vec{\Phi}(z)$  is defined using Bloch theorem as

$$\vec{\Phi}(z) = e^{iQz} \begin{bmatrix} U_E(z) \\ U_B(z) \end{bmatrix} \quad (10)$$

where  $U_{E,B}(z)$  have the same periodicity as the periodic uniform array, and  $Q$  is a complex number in general. Considering the fact that the factor  $\exp(-iQz)$  is the same for both electric ( $E$ ) and magnetic ( $B$ ) fields in an e.m wave, we can write

$$1 - (T_{11} + T_{22})e^{iQd} + e^{2iQd} = 0 \quad (11)$$

where  $T_{ij}$  are the elements of the matrix  $T_d$ . Multiplying each term by  $\exp(-iQd)$ , we finally obtain:

$$\cos Qd = (T_{11} + T_{22})/2 \quad (12)$$

A Bragg mirror is essentially a periodic structure composed of pairs of layers of dielectric or semiconductor materials characterized by media with different refractive indices (say  $n_a$  and  $n_b$ ). The thicknesses of the layers ( $a$  and  $b$ , respectively) are chosen so that

$$n_a a = n_b b \equiv \bar{\lambda}/4 \quad (13)$$

Eq. (13) is known as Bragg interference condition. Under normal incident light wave, the transfer matrices across the layers that compose the grating are:

$$\hat{T}_a = \begin{bmatrix} \cos k_a a & \frac{i}{n_a} \sin k_a a \\ i n_a \sin k_a a & \cos k_a a \end{bmatrix}, \hat{T}_b = \begin{bmatrix} \cos k_b b & \frac{i}{n_b} \sin k_b b \\ i n_b \sin k_b b & \cos k_b b \end{bmatrix} \quad (14)$$

where  $k_a = \omega n_a / c$ ,  $k_b = \omega n_b / c$ . The transfer matrix  $T$  across the period of the mirror is their corresponding product which is given as:

$$\hat{T} = \hat{T}_b \hat{T}_a \quad (15)$$

An infinite Bragg mirror represents the simplest one-dimensional photonic dielectric structure. Its band structure is given by Eq. (12). Its solutions with the real  $Q$  form the set of allowed photonic bands, contrary to which the solutions obtained from complex  $Q$  having a non-zero imaginary part form photonic gaps or stop-bands. At the centre frequency of the stop-band, we have

$$\hat{T} = \begin{bmatrix} -\frac{n_a}{n_b} & 0 \\ 0 & -\frac{n_b}{n_a} \end{bmatrix} \quad (16)$$

The eigenvalues are:

$$\exp[iQ(a+b)] = -\frac{n_a}{n_b}, \exp[-iQ(a+b)] = -\frac{n_b}{n_a} \quad (17)$$

Reflection coefficient of a Bragg mirror with a semi-definite structure at gives

$$\hat{T} = - \begin{bmatrix} \frac{n_a}{n_b} & i \left( \frac{1}{n_a} + \frac{1}{n_b} \right) x \\ i(n_a + n_b)x & \frac{n_b}{n_a} \end{bmatrix} \quad (18)$$

Thus reflection and transmission coefficients at the centre of the photonic band gap may be written as:

$$\bar{r} = \frac{\left( \frac{n_b}{n_a} \right)^{2N} - \frac{n_f}{n_0}}{\left( \frac{n_b}{n_a} \right)^{2N} + \frac{n_f}{n_0}} \quad (19.1)$$

$$\bar{t} = \frac{2 \left( -\frac{n_b}{n_a} \right)^N}{\left( \frac{n_b}{n_a} \right)^{2N} + \frac{n_f}{n_0}} \quad (19.2)$$

where  $N$  is the number of periods in the grating, and  $n_f$  is the refractive index behind the grating, and

$$\text{Refractive Index Contrast Ratio} = \frac{n_b}{n_a} \quad (20)$$

### 3. Results & Discussion

Using Eq. (19.1), Eq. (19.2) and Eq. (20), stopband width of the photonic crystal structure is computed and plotted as a function of wavelength. It increases with increase in the contrast between

the two refractive indices. Fig 1 shows the reflectivity of the Bragg gratings which is made of different semiconductor and dielectric materials but all having  $\lambda=1550$  nm.

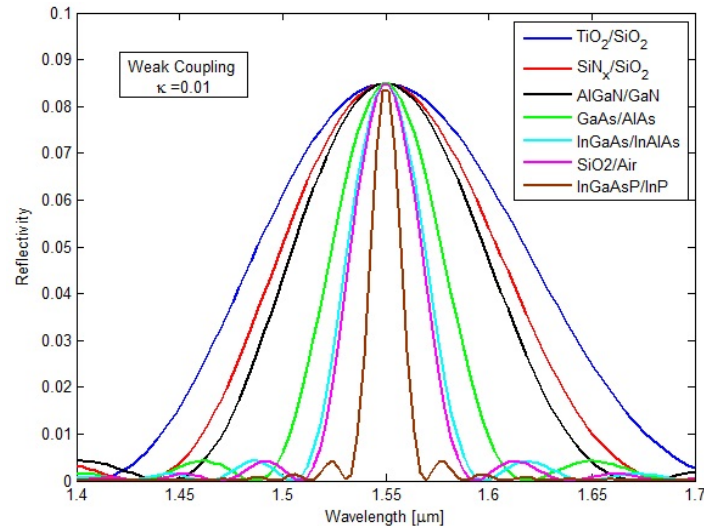


**Fig 1:** Photonic bandwidth for different material composition under weak coupling between forward and backward propagating wave

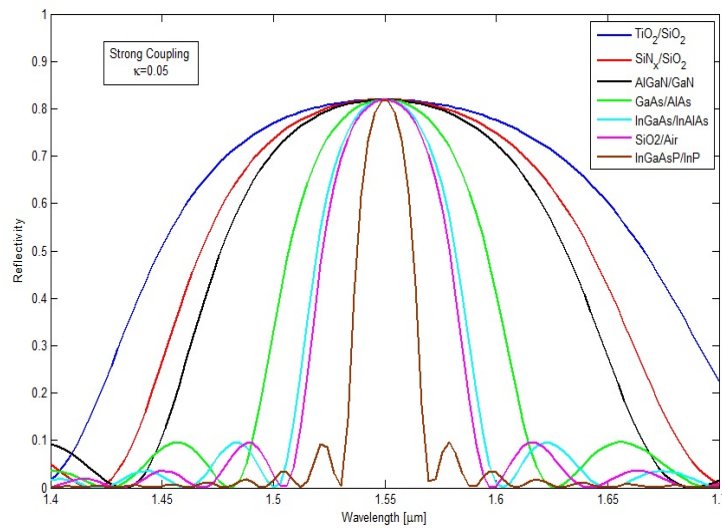


**Fig 2:** Photonic bandwidth for different material composition under strong coupling between forward and backward propagating wave

Following table shows the computed result for different material compositions:

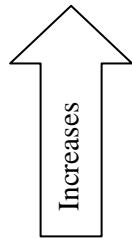
Material Composition	Refractive Index Contrast Ratio	Width of the Photonic band-gap
TiO <sub>2</sub> /SiO <sub>2</sub>	0.8687	<div style="text-align: center;">  </div>
SiN <sub>x</sub> /SiO <sub>2</sub>	0.7815	
AlGaIn/GaN	0.7530	
GaAs/AlAs	0.5866	
InGaAs/InAlAs	0.3182	
SiO <sub>2</sub> /Air	0.0761	
InGaAsP/InP	0.0223	

Fig. 1 shows the reflectivity profile i.e. the photonic bandgap width for different material compositions under weak coupling conditions. It is evident from the plot that with the increase in contrast ratio between the two materials with refractive index  $n_a$  and  $n_b$ , the better is the response of reflectivity of the grating. Fig. 2 shows a similar plot under strong coupling between the forward and backward wave. In this case, effective width of the photonic bandgap increases. Thus under strong coupling, it becomes easy to tailor the photonic bandgap.

#### **4. Conclusion**

Eigenmodes, reflectivity, transmittivity and refractive index contrast ratio for the multilayer 1D photonic crystal structure is analytically computed. Contrast ratio is calculated for different material system to measure the extent of photonic bandwidth. It is observed from the result that with increase of the ratio, photonic bandwidth increases. The width can be tuned by changing the coupling coefficient between forward and backward propagating waves, and under strong coupling condition, tailoring of bandwidth is more flexible. Result is computed at 1550 nm for optical communication applications.

#### **References**

- [1] E. Yablonovitch, "Inhibited spontaneous emission in solid-state physics and electronics", *Physical Review Letters*, vol. 58, pp. 2059-2061, 1987.
- [2] R. Loudon, "The Propagation of Electromagnetic Energy through an Absorbing Dielectric" *Journal of Physics A*, vol. 3, pp. 233-245, 1970.
- [3] D. Mao, Z. Ouyang, J. C. Wang, "A Photonic-Crystal Polarizer Integrated with the Functions of Narrow Bandpass and Narrow Transmission Angle Filtering", *Applied Physics B*, vol. 90, pp. 127-131, 2008.
- [4] A. Adibi, "Role of distributed Bragg reflection in photonic-crystal optical waveguides", *Physical Review B*, vol. 64, p. 041102, 2001.
- [5] E. Ozbay, "Layer-by-layer photonic crystals from microwave to far-infrared frequencies", *Journal of Optical Society of America B*, vol. 13, pp. 1945-1955, 1996.
- [6] J. Limpert, T. Schreiber, S. Nolte, H. Zellmer, T. Tunnermann, R. Iliew, F. Lederer, J. Broeng, G. Vienne, A. Petersson, C. Jakobsen, "High Power Air-Clad Large-Mode-Area Photonic Crystal Fiber Laser", *Optic Express*, vol. 11, pp. 818-823, 2003.
- [7] J. Hansryd, P. A. Andrekson, M. Westlund, J. Li, P. O. Hedekvist, "Fiber-based Optical Parametric Amplifiers and their Applications", *IEEE Journal of Selected Topics on Quantum Electronics*, vol. 8, pp. 506- 520, 2002.
- [8] P. Szczepanski, "Semiclassical Theory of Multimode Operation of a Distributed Feedback Laser", *IEEE Journal of Quantum Electronics*, vol. 24, pp. 1248-1257, 1988.
- [9] J. C. Chen, H. A. Haus, S. Fan, P. R. Villeneuve, J. D. Joannopoulos, "Optical Filters from Photonic Band Gap Air Bridges", *Journal of Lightwave Technology*, vol. 14, pp. 2575-2580, 1996.
- [10] A. Mekis, J. C. Chen, I. Kurland, S. Fan, P. R. Villeneuve, J. D. Joannopoulos, "High Transmission Optical Filters from Photonic Band Gap Air Bridges", *Physical Review Letters*, vol. 77, pp. 3787-3790, 1996.
- [11] R. Hillebrand, W. Hergert, W. Harm, "Theoretical Bandgap Studies of Two Dimensional Photonic Crystals with Varying Column Roundness", *Physica Status Solidi (b)*, vol. 217, pp. 981-989, 2000.
- [12] D. G. Popescu, P. Sterian, "Photonic Crystal Fiber Mode Characterization With Multipole Method", *Journal of Advanced Research in Physics*, vol. 2, p. 021105, 2011.
- [13] J. Zhao, X. Li, L. Zhong, G. Chen, *Journal of Physics: Conference Series (Dielectrics 2009: Measurement Analysis and Applications, 40th Anniversary Meeting)*, vol. 183, p. 012018, 2009.

- [14] H. Meny, N. C. Nguyenz, R. M. Freundx, P. A. Parrilo, J. Perairek, “Bandgap Optimization of Two Dimensional Photonic Crystals Using Semi-definite programming and Subspace Methods”, arXiv: 0907.2267 v1 [math.OC], 13 Jul 2009.
- [15] S. Preblea, M. Lipson, “ Two Dimensional Photonic Crystals designed by Evolutionary Algortihms”, Applied Physics Letters, vol. 86, p. 061111, 2005.
- [16] C. Y. Kao, S. Osher, E. Yablonovitch, “ Maximizing Bandgaps in Two-Dimensional Photonic Crystals by Using Level Set Methods”,white paper.